

# A Fully Self-Consistent Treatment of Collective Fluctuations in Quantum Liquids

Eran Rabani

*School of Chemistry, The Sackler Faculty of Exact Sciences, Tel Aviv University, Tel Aviv 69978, Israel*

and

David R. Reichman

*Department of Chemistry and Chemical Biology, Harvard University, Cambridge, MA 02138*

(Dated: May 22, 2019)

The problem of calculating collective density fluctuations in quantum liquids is revisited. A fully quantum mechanical self-consistent treatment based on a quantum mode-coupling theory [E. Rabani and D.R. Reichman, *J. Chem. Phys.* **116**, 6271 (2002)] is presented. The theory is compared with the maximum entropy analytic continuation approach and with available experimental results. The quantum mode-coupling theory provides semi-quantitative results for both short and long time dynamics. The proper description of long time phenomena is important in future study of problems related to the physics of glassy quantum systems, and to the study of collective fluctuations in Bose fluids.

## I. INTRODUCTION

The study of the dynamical properties of quantum liquids has a storied history.<sup>1</sup> The interplay of nuclear dynamics, particle statistics, dimensionality, disorder and temperature can lead to, or suppress, dramatic effects such as superfluidity in <sup>4</sup>He and superconductivity in the superfluid Fermi liquid state of conducting electrons in metals.<sup>2</sup> Due to the great computational difficulties presented by a direct assault on the real-time many-body Schrödinger equation, microscopic approaches to calculate the frequency dependent response in condensed phase disordered quantum systems are approximate and generally rely on somewhat uncontrolled approximations.

One approach that has been useful in a variety of physical contexts is the analytic continuation of numerically exact imaginary time path-integral data.<sup>3,4</sup> This approach has been fruitful for the study of quantum impurity models such as the Anderson Hamiltonian,<sup>5</sup> as well as models of correlated electrons such as the Hubbard Hamiltonian.<sup>6</sup> Berne and coworkers have successfully applied the maximum entropy (MaxEnt) version of analytic continuation to study the dynamics of electrons in simple liquids,<sup>7,8</sup> vibrational and electronic relaxation of impurities in liquid and solid hosts,<sup>9,10</sup> and adiabatic rate constants in condensed phase environments.<sup>11,12</sup> Boninsegni and Ceperley have applied MaxEnt to study the dynamic structure factor of liquid <sup>4</sup>He above and below the  $\lambda$ -transition.<sup>13</sup> For the normal state, they find good agreement with experimental results, while the agreement is significantly worse in the superfluid state. In particular, sharp quasiparticle peaks are not well resolved with the MaxEnt approach.<sup>13</sup> This failure arises from the intrinsic ill-posed nature of the numerical continuation to the real-time axis. The conditioning of the data which helps alleviate numerical instabilities makes the differentiation of fine energy scales difficult, resulting in smoothing of the response functions.

In several recent papers,<sup>14,15,16,17,18</sup> we have explored a molecular hydrodynamic approach for calculating the dynamic response functions of quantum liquids. In particular, we have formulated a detailed generalization of the classical mode-coupling approach to the quantum case.<sup>16</sup> We have studied both single particle as well as collective fluctuations, with good agreement with recent experiments performed on liquid *para*-hydrogen<sup>19,20,21,22,23</sup> and liquid *ortho*-deuterium.<sup>24,25,26</sup> Unlike the MaxEnt technique, our approach is a *theory* and thus provides additional insight into the dynamics of quantum liquids. This fact implies several additional advantages. First, because our theory is the direct analog of the approach used in the study of quantum spin glasses,<sup>27,28,29</sup> interesting connections between quantum systems with and without quenched disorder may be made. For example, our recent study of the spectrum of density fluctuations in liquid *para*-hydrogen, where finite frequency quasiparticle peaks appear in the dynamic structure factor,  $S(q, \omega)$ , resonates with the general result of Cugliandolo and Lozano that "trivial" quantum fluctuations add coherence to the decay of dynamics correlators at short-times.<sup>30</sup> Furthermore, in principle we could study a range of problems related to the physics of glassy quantum systems, including the aging behavior of an out-of-equilibrium quantum liquid.<sup>27,28,29</sup> Because the MaxEnt approach relies implicitly on the equilibrium formulation of quantum statistical mechanics, this approach cannot be used to investigate such questions.

In order to study such interesting problems, as well as the challenges imposed by nontrivial collective behavior exhibited, for example, by superfluid <sup>4</sup>He, we need to further develop our theoretical apparatus. In our previous studies, we imposed self-consistency in the study of single-particle properties, but not in the more difficult case of collective properties such as the dynamics of density fluctuations.<sup>14,17,18</sup> In this work, we make several accurate and physically motivated approximations that render the formal equations presented in Ref.

16 amenable to direct numerical investigation. We revisit the problem of the study of  $S(q, \omega)$  in liquid *ortho*-deuterium and *para*-hydrogen, and show that a fully self-consistent treatment of density fluctuations greatly improves the agreement between the low frequency behavior seen in experiments and corrects the behavior of our previously used quantum viscoelastic theory.<sup>14,17,18</sup> This low frequency behavior associated with the long time relaxation of density fluctuations in these liquids is not well captured by the MaxEnt approach.

Our paper is organized as follows: In section II we provide an overview of our self-consistent quantum mode-coupling approach to density fluctuations in quantum liquids. Furthermore, we discuss the improvements of the present approach and the physical approximation that are introduced to make our current study amenable to path integral Monte Carlo (PIMC) simulation techniques. In section III we discuss the MaxEnt approach used in the present study. Results for collective density fluctuations in liquids *ortho*-deuterium and *para*-hydrogen is presented in section IV. We compare the predictions of our quantum mode-coupling theory to the MaxEnt results and also to available experimental results. Finally, in section V we conclude.

## II. SELF-CONSISTENT QUANTUM MODE-COUPLING THEORY

In this section we provide a short overview of our quantum mode-coupling approach suitable for the study of collective density fluctuations in quantum liquids.<sup>14,15,16,17,18</sup> For reasons discussed in Ref. 16, our formulation of the quantum mode-coupling theory (QMCT) is based on the Kubo transform of the dynamical correlation function of interest. For collective density fluctuations the experimental measured quantity is the dynamic structure factor,  $S(q, \omega)$ , which is related to the Kubo transform of the intermediate scattering function,  $F^\kappa(q, t)$  by:

$$S(q, \omega) = \frac{\beta\hbar\omega}{2} \left\{ \coth\left(\frac{\beta\hbar\omega}{2}\right) + 1 \right\} S^\kappa(q, \omega) \quad (1)$$

where the Kubo transform of the dynamic structure factor is given in terms of a Fourier transform of the Kubo transform of the intermediate scattering function:

$$S^\kappa(q, \omega) = \int_{-\infty}^{\infty} dt e^{i\omega t} F^\kappa(q, t). \quad (2)$$

In the above equations  $\beta = \frac{1}{k_B T}$  is the inverse temperature, and the superscript  $\kappa$  is a shorthand notation of the Kubo transform (to be described below). The quantum mode-coupling theory described in this section provides a set of closed, self-consistent equations for  $F^\kappa(q, t)$ , which can be used to generate the dynamic structure factor using the above transformations.

We begin with the definition of two dynamical variables, the quantum collective density operator

$$\hat{\rho}_{\mathbf{q}} = \sum_{\alpha=1}^N e^{i\mathbf{q} \cdot \hat{\mathbf{r}}_{\alpha}}, \quad (3)$$

and the longitudinal current operator

$$\hat{j}_{\mathbf{q}} = \frac{1}{2m|q|} \sum_{\alpha=1}^N [(\mathbf{q} \cdot \hat{\mathbf{p}}_{\alpha}) e^{i\mathbf{q} \cdot \hat{\mathbf{r}}_{\alpha}} + e^{i\mathbf{q} \cdot \hat{\mathbf{r}}_{\alpha}} (\hat{\mathbf{p}}_{\alpha} \cdot \mathbf{q})], \quad (4)$$

where  $\hat{\mathbf{r}}_{\alpha}$  is the position vector operator of particle  $\alpha$  with a conjugate momentum  $\hat{\mathbf{p}}_{\alpha}$  and mass  $m$ , and  $N$  is the total number of liquid particles. The quantum collective density operator and the longitudinal current operator satisfy the continuity equation  $\dot{\hat{\rho}}_{\mathbf{q}} = iq\hat{j}_{\mathbf{q}}$ , where the dot denotes a time derivative, i.e.  $\dot{\hat{\rho}}_{\mathbf{q}} = \frac{i}{\hbar} [\hat{H}, \hat{\rho}_{\mathbf{q}}]$ .

Following the standard projection operator procedure,<sup>31,32,33,34</sup> the time evolution of the Kubo transform of the intermediate scattering function,  $F^\kappa(q, t) = \frac{1}{N} \langle \hat{\rho}_{\mathbf{q}}^\dagger, \hat{\rho}_{\mathbf{q}}^\kappa(t) \rangle$  ( $\langle \dots \rangle$  denote a quantum mechanical ensemble average), is given by the exact quantum generalized Langevin equation

$$\ddot{F}^\kappa(q, t) + \omega_\kappa^2(q) F^\kappa(q, t) + \int_0^t dt' K^\kappa(q, t - t') \dot{F}^\kappa(q, t') = 0, \quad (5)$$

where (as noted above) the notation  $\kappa$  implies that the quantity under consideration involves the Kubo transform given by<sup>35</sup>

$$\hat{\rho}_{\mathbf{q}}^\kappa = \frac{1}{\beta\hbar} \int_0^{\beta\hbar} d\lambda e^{-\lambda\hat{H}} \hat{\rho}_{\mathbf{q}} e^{\lambda\hat{H}}, \quad (6)$$

and  $\hat{H}$  is the Hamiltonian operator of the system. In the above equation  $\omega_\kappa^2(q)$  is the Kubo transform of the frequency factor given by:

$$\omega_\kappa^{2n}(q) = \frac{1}{S^\kappa(q)} \left\langle \frac{d^n \hat{\rho}_{\mathbf{q}}^\dagger}{dt^n}, \frac{d^n \hat{\rho}_{\mathbf{q}}^\kappa}{dt^n} \right\rangle \quad (7)$$

with  $S^\kappa(q) = F^\kappa(q, 0) = \frac{1}{N} \langle \hat{\rho}_{\mathbf{q}}^\dagger, \hat{\rho}_{\mathbf{q}}^\kappa(0) \rangle$  being the Kubo transform of the static structure factor. The Kubo transform of the memory kernel appearing in Eq. (5) is related to the Kubo transform of the random force  $\hat{R}_{\mathbf{q}} = \frac{d\hat{j}_{\mathbf{q}}}{dt} - i|q| \frac{J^\kappa(q)}{S^\kappa(q)} \hat{\rho}_{\mathbf{q}}$ , and is formally given by

$$J^\kappa(q, t) = \frac{1}{N J^\kappa(q)} \langle \hat{R}_{\mathbf{q}}^\dagger, e^{i(1-\mathcal{P}^\kappa)\hat{\mathcal{L}}t} \hat{R}_{\mathbf{q}}^\kappa \rangle, \quad (8)$$

where  $J^\kappa(q) = \frac{1}{N} \langle \hat{j}_{\mathbf{q}}^\dagger, \hat{j}_{\mathbf{q}}^\kappa(0) \rangle$  is the Kubo transform of the zero time longitudinal current correlation function,  $\hat{\mathcal{L}} = \frac{1}{\hbar} [\hat{H}, \cdot]$  is the quantum Liouville operator, and  $\mathcal{P}^\kappa = \frac{\langle \hat{A}^\dagger, \cdot \rangle}{\langle \hat{A}^\dagger, \hat{A}^\kappa \rangle} \hat{A}^\kappa$  is the projection operator used to derive Eq. (5) with the row vector operator given by  $\hat{A} = (\hat{\rho}_{\mathbf{q}}, \hat{j}_{\mathbf{q}})$ .

To reduce the complexity of solving Eq. (8) we follow the lines of classical mode-coupling theory<sup>36,37,38</sup> to obtain a closed expression for the memory kernel.<sup>16</sup> We use the approximate form  $K^\kappa(q, t) = K_f^\kappa(q, t) + K_m^\kappa(q, t)$  where the “quantum binary” portion  $K_f^\kappa(q, t)$  and the quantum mode-coupling portion  $K_m^\kappa(q, t)$  are obtained using the standard classical procedure,<sup>36,37,38</sup> but with a proper quantum mechanical treatment.

The fast decaying binary term is determined from a short-time expansion of the exact Kubo transform of the memory function, and is given by

$$K_f^\kappa(q, t) = K^\kappa(q, 0) \exp\{-(t/\tau^\kappa(q))^2\}, \quad (9)$$

where the lifetime is approximated by<sup>39</sup>

$$\tau^\kappa(q) = [3K^\kappa(q, 0)/4]^{-1/2}. \quad (10)$$

In the above equations  $K^\kappa(q, 0)$  is the zero time moments of the memory kernel given by

$$K^\kappa(q, 0) = \frac{\omega_\kappa^4(q)}{\omega_\kappa^2(q)} - \omega_\kappa^2(q), \quad (11)$$

where  $\omega_\kappa^{2n}(q)$  is given in Eq. (7). Note that the exact expression for the lifetime involves higher order terms such as  $\omega_\kappa^6(q)$  and is given by  $\tau^\kappa(q) = [-\ddot{K}^\kappa(q, 0)/2K^\kappa(q, 0)]^{-1/2}$ , where  $\ddot{K}^\kappa(q, 0) = -\omega_\kappa^6(q)/\omega_\kappa^4(q) + (\omega_\kappa^4(q)/\omega_\kappa^2(q))^2$ . Although the calculation of  $\omega_\kappa^6(q)$  is possible it involves higher order derivative of the interaction potential and thus becomes a tedious task for the path integral Monte Carlo technique. Interestingly, we find that the approximation to the lifetime given by Eq. (10) is accurate to within 5 percent for classical fluids. Thus, we use this simpler approximate lifetime also for the quantum systems studied here.

The slow decaying mode-coupling portion of the memory kernel,  $K_m^\kappa(q, t)$ , must be obtained from a quantum mode-coupling approach. The basic idea behind this approach is that the random force projected correlation function, which determines the memory kernel for the intermediate scattering function (cf. Eq. (8)), decays at intermediate and long times predominantly into modes which are associated with quasi-conserved dynamical variables. It is reasonable to assume that the decay of the memory kernel at long times will be governed by those modes that have the longest relaxation time. The slow decay is basically attributed to couplings between wavevector-dependent density modes of the form

$$\hat{B}_{\mathbf{k}, \mathbf{q}-\mathbf{k}} = \hat{\rho}_{\mathbf{k}} \hat{\rho}_{\mathbf{q}-\mathbf{k}}, \quad (12)$$

where translational invariance of the system implies that the only combination of densities whose inner product with a dynamical variable of wavevector  $-\mathbf{q}$  is nonzero is  $\hat{\rho}_{\mathbf{k}}$  and  $\hat{\rho}_{\mathbf{q}-\mathbf{k}}$ .

After some tedious algebra the slow mode-coupling portion of the memory kernel can be approximated

by<sup>15,16</sup>

$$K_m^\kappa(q, t) \approx \frac{2}{(2\pi)^3 n J^\kappa(q)} \int d\mathbf{k} |V^\kappa(\mathbf{q}, \mathbf{k})|^2 \times [F^\kappa(k, t) F^\kappa(|\mathbf{q} - \mathbf{k}|, t) - F_b^\kappa(k, t) F_b^\kappa(|\mathbf{q} - \mathbf{k}|, t)], \quad (13)$$

where  $n$  is the number density. The binary term of the Kubo transform of the intermediate scattering function,  $F_b^\kappa(q, t)$ , is obtained from a short time expansion of  $F^\kappa(q, t)$  similar to the *exact* expansion used for the binary term of  $K^\kappa(q, t)$ , and is given by

$$F_b^\kappa(q, t) = S^\kappa(q) \exp\left\{-\frac{1}{2}\omega_\kappa^2(q)t^2\right\}. \quad (14)$$

The subtraction of the product of terms in Eq. (13) involving  $F_b^\kappa(q, t)$  is done to prevent over-counting the total memory kernel at short times, namely, to ensure that the even time moments of the total memory kernel are exact to forth order in time.

The vertex in Eq. (13) is formally given by

$$V^\kappa(\mathbf{q}, \mathbf{k}) = \frac{1}{2N} \left( \frac{\langle \frac{d}{dt} \hat{j}_\mathbf{q}^\dagger, \hat{\rho}_\mathbf{k}^\kappa \hat{\rho}_{\mathbf{q}-\mathbf{k}}^\kappa \rangle}{S^\kappa(k) S^\kappa(|\mathbf{q} - \mathbf{k}|)} - i|q| \frac{J^\kappa(q)}{S^\kappa(q)} \frac{\langle \hat{\rho}_\mathbf{q}^\dagger \hat{\rho}_\mathbf{k}^\kappa \hat{\rho}_{\mathbf{q}-\mathbf{k}}^\kappa \rangle}{S^\kappa(k) S^\kappa(|\mathbf{q} - \mathbf{k}|)} \right), \quad (15)$$

involving a double Kubo transform.<sup>40</sup> In the applications reported below we have calculated the vertex using the following approximations for the three point correlation functions. For  $\langle \hat{\rho}_\mathbf{q}^\dagger \hat{\rho}_\mathbf{k}^\kappa \hat{\rho}_{\mathbf{q}-\mathbf{k}}^\kappa \rangle$  the (Kubo) convolution approximation has been developed,<sup>41</sup> leading to:

$$\frac{1}{N} \langle \hat{\rho}_\mathbf{q}^\dagger \hat{\rho}_\mathbf{k}^\kappa \hat{\rho}_{\mathbf{q}-\mathbf{k}}^\kappa \rangle \approx S(k) S^\kappa(|\mathbf{q} - \mathbf{k}|) S^\kappa(q), \quad (16)$$

while for  $\langle \frac{d}{dt} \hat{j}_\mathbf{q}^\dagger, \hat{\rho}_\mathbf{k}^\kappa \hat{\rho}_{\mathbf{q}-\mathbf{k}}^\kappa \rangle$  we have used the fact that the Kubo transform  $J^\kappa(q) = \frac{1}{N} \langle \hat{j}_\mathbf{q}^\dagger, \hat{j}_\mathbf{q}^\kappa(0) \rangle$  can be approximated by  $k_B T/m$ ,  $m$  being the mass of the particle, within an error that is less than one percent for the relevant  $q$  values studied in this work. Based on this fact, we approximate  $\langle \frac{d}{dt} \hat{j}_\mathbf{q}^\dagger, \hat{\rho}_\mathbf{k}^\kappa \hat{\rho}_{\mathbf{q}-\mathbf{k}}^\kappa \rangle$  by:

$$\frac{1}{N} \left\langle \frac{d}{dt} \hat{j}_\mathbf{q}^\dagger, \hat{\rho}_\mathbf{k}^\kappa \hat{\rho}_{\mathbf{q}-\mathbf{k}}^\kappa \right\rangle \approx -\frac{k_B T}{mq} (\mathbf{q} \cdot \mathbf{k} S^\kappa(|\mathbf{q} - \mathbf{k}|) + (\mathbf{q} - \mathbf{k}) \cdot \mathbf{q} S^\kappa(k)). \quad (17)$$

The combination of these approximations lead to a simplified vertex given by

$$V^\kappa(\mathbf{q}, \mathbf{k}) \approx \frac{i k_B T}{2mq} \left( \frac{\mathbf{q} \cdot \mathbf{k}}{S^\kappa(k)} + \frac{(\mathbf{q} - \mathbf{k}) \cdot \mathbf{q}}{S^\kappa(|\mathbf{q} - \mathbf{k}|)} - q^2 \frac{S(k)}{S^\kappa(k)} \right), \quad (18)$$

where  $S(k)$  is the quantum mechanical static structure factor (non Kubo transformed version). At high values

of  $k$  the vertex should decay to zero, while the approximation fails to do so. Hence, in the applications discussed below we employ a  $k$ -cutoff to overcome the shortcoming of our approximation. Below we discuss the choice of  $k_{cut}$  for the two model systems studied.

To obtain the Kubo transform of the intermediate scattering function, one requires as input the frequency factor  $\omega_\kappa^2(q)$ , and the memory kernel  $K^\kappa(q, t)$ . Since the memory kernel depends on  $F^\kappa(q, t)$ , the equation of motion for the intermediate scattering function (Eq. (5)) must be solved self-consistently. The time-independent terms in the memory kernel, and the frequency factor can be obtained from *static* equilibrium input using a suitable path integral Monte Carlo scheme.<sup>16,42</sup>

### III. ANALYTIC CONTINUATION OF THE INTERMEDIATE SCATTERING FUNCTION

An alternative approach to the quantum mode-coupling theory is based on the numerical maximum entropy analytic continuation approach, which has recently been used by Boninsegni and Ceperley to study density fluctuations in liquid helium.<sup>13</sup> In this section we provide a short outline of maximum entropy analytic continuation approach applicable to study collective density fluctuations in quantum liquids.

The analytic continuation of the intermediate scattering function is based on the Fourier relation between  $S(q, \omega)$  and  $F(q, t)$ :

$$F(q, t) = \frac{1}{2\pi} \int_{-\infty}^{\infty} d\omega e^{-i\omega t} S(q, \omega). \quad (19)$$

The dynamic structure factor is thus analogous to the spectral density used in the analytic continuation of spectral line shapes<sup>7,8</sup> and to the frequency dependent rate constant or diffusion constant used in analytic continuation of rates.<sup>11,43</sup> By performing the replacement  $t \rightarrow -i\tau$ , and using the detailed balance relation  $S(q, -\omega) = e^{-\beta\omega} S(q, \omega)$  we obtain

$$\tilde{F}(q, \tau) = \frac{1}{2\pi} \int_0^{\infty} d\omega \left[ e^{-\omega\tau} + e^{(\tau-\beta)\omega} \right] S(q, \omega), \quad (20)$$

where  $t, \tau \geq 0$ , and

$$\tilde{F}(q, \tau) = \frac{1}{Z} \frac{1}{N} \text{Tr} \left( e^{-\beta H} e^{\tau H} \hat{\rho}_q^\dagger e^{-\tau H} \hat{\rho}_q \right). \quad (21)$$

The reason for introducing the imaginary time intermediate scattering function,  $\tilde{F}(q, \tau)$ , is that, unlike its real time counterpart, it is straightforward to obtain it using an appropriate path-integral Monte Carlo simulation technique.<sup>44,45</sup> However, in order to obtain the dynamic structure factor and the real time intermediate scattering function one has to invert the integral in Eq. (20). Due to the singular nature of the integration kernel the inversion of Eq. (20) is an ill-posed problem. As a consequence, a direct approach to the inversion would lead

to an uncontrollable amplification of the statistical noise in the data for  $\tilde{F}(q, \tau)$ , resulting in an infinite number of solutions that satisfy Eq. (20). Clearly, in this case, little can be said about the real time dynamics and the corresponding dynamic structure factor.

In recent years, Bayesian ideas have been used to deal with the ill-posed nature of continuing the noisy imaginary time Monte Carlo data to real time.<sup>3,4</sup> One of the most widely used approaches is the maximum entropy method.<sup>4,46</sup> The method requires only that the transformation which relates the data and the solution be known. Furthermore, maximum entropy allows the inclusion of prior knowledge about the solution in a logically consistent fashion. As such, the method is well-suited for solving ill-posed mathematical problems.

In the language of the maximum entropy method  $\tilde{F}(q, \tau)$  is the data,  $K(\tau, \omega) = e^{-\omega\tau} + e^{(\tau-\beta)\omega}$  is the singular kernel, and  $S(q, \omega)$  is the solution, also referred to as the map. Maximum entropy principles provide a way to choose the most probable solution which is consistent with the data through the methods of Bayesian inference. Typically, the data is known only at a discrete set of points  $\{\tau_j\}$ , and thus we search for the solution at a discrete set of points  $\{\omega_l\}$ . The maximum entropy method selects the solution which maximizes the posterior probability, or the probability of the solution  $S(q, \omega_l)$  given a data set  $\tilde{F}(q, \tau_j)$ . The posterior probability is given by<sup>46</sup>

$$\mathcal{P}(S(q, \omega) | \tilde{F}(q, \tau)) \propto \exp(\alpha_q S_q - \chi_q^2/2). \quad (22)$$

Here  $\chi_q^2$  is the standard mean squared deviation from the data, and  $S_q$  is the information entropy.<sup>43</sup>

Obtaining the maximum entropy solution then involves finding a map  $S(q, \omega)$  which maximizes the posterior probability and is therefore a maximization problem in  $M$  variables, where  $M$  is the number of points  $\{\omega_l\}$  at which the solution is evaluated. The solution obtained in this way is still conditional on the arbitrary parameter  $\alpha_q$ , which can be interpreted as a regularization parameter. In this work, we use a flat default map that satisfies a known sum rule, such as the integral over  $S(q, \omega)$ , and  $\alpha_q$  is selected according to the L-curve method.<sup>47</sup> In this case we regard  $\alpha_q$  as a regularization parameter controlling the degree of smoothness of the solution, and entropy as the regularizing function. The value of  $\alpha_q$  is selected by constructing a plot of  $\log[-S_q(S(q, \omega))]$  vs.  $\log \chi_q^2$ . This curve has a characteristic L-shape, and the corner of the L, or the point of maximum curvature, corresponds to the value of  $\alpha_q$  which is the best compromise between fitting the data and obtaining a smooth solution.

## IV. RESULTS

Although it is known that liquid *ortho*-deuterium and liquid *para*-hydrogen may be treated as Boltzmann particles without the complexity of numerically treating par-

ticle statistics,<sup>48</sup> they still exhibits some of the hallmarks of a highly quantum liquid. In fact, recent theoretical<sup>14,15,16,17,18,21,23,43,49,50,51</sup> and experimental studies<sup>19,20,21,22,26</sup> show that these dense liquids are characterized by quantum dynamical susceptibilities which are not reproducible using classical theories. Thus, these liquids are ideal to assess the accuracy of methods developed for quantum liquids such as the self consistent quantum mode-coupling theory and the maximum entropy analytic continuation approach.

Here we report on a direct comparison between these methods for collective density fluctuations in liquid *ortho*-deuterium and liquid *para*-hydrogen. A comparison between the two approaches has been made for self-transport in liquid *para*-hydrogen<sup>43</sup> where good agreement has been observed for the real time velocity autocorrelation function. However, the present comparison is more challenging since the experimental dynamic structure factor for these liquids is characterized by more than a single frequency peak (unlike the case of self-transport),<sup>20,26</sup> indicating that more than a single timescale is involved in the relaxation of the density fluctuations. So far, in the context of our molecular hydrodynamic approach, density fluctuations in these dense liquids has been described only within the quantum viscoelastic model<sup>14,17,18</sup> which fails to reproduce the low frequency peak in  $S(q, \omega)$  that is associated with long time dynamics. Therefore, one challenge for the improved self-consistent quantum hydrodynamic approach and for the analytic continuation method is to recover this long time behavior.

### A. Technical details

To obtain the static input required by the quantum mode-coupling theory and the imaginary time intermediate scattering function required for the analytic continuation approach we have performed PIMC simulations at  $T = 20.7\text{K}$  and  $\rho = 0.0254\text{\AA}^{-3}$  for liquid *ortho*-deuterium<sup>25</sup> and  $T = 14\text{K}$  and  $\rho = 0.0235\text{\AA}^{-3}$  for liquid *para*-hydrogen.<sup>52</sup> The PIMC simulations were done using the NVT ensemble with 256 particles interacting via the Silvera-Goldman potential,<sup>53,54</sup> where the entire molecule is described as a spherical particle, so the potential depends only on the radial distance between particles. The staging algorithm<sup>55</sup> for Monte Carlo chain moves was employed to compute the numerically exact input. The imaginary time interval was discretized into  $P$  Trotter slices of size  $\epsilon = \beta/P$  with  $P = 20$  and  $P = 50$  for liquid *ortho*-deuterium and liquid *para*-hydrogen, respectively. Approximately  $2 \times 10^6$  Monte Carlo passes were made, each pass consisted of attempting moves in all atoms and all the beads that were staged. The acceptance ratio was set to be approximately 0.25 – 0.3 for both liquids.

The static input obtained from the PIMC simulations was then used to generate the memory kernel ( $K^\kappa(q, t) =$

$K_f^\kappa(q, t) + K_m^\kappa(q, t))$ ) and frequency factor ( $\omega_\kappa^2(q)$ ) needed for the solution of the equations of motion for  $F^\kappa(q, t)$ . To obtain  $K_m^\kappa(q, t)$  we solved Eq. (13) with a cutoff in  $k$  to overcome the divergent behavior discussed above (cf. Eq. (18)). The choice of  $k_{cut}$  is straightforward given that the approximate vertex decays to zero at intermediate  $k$  values before the unphysical divergent behavior steps in. We have used  $k_{cut} = 5.66\text{\AA}^{-1}$  and  $k_{cut} = 4.73\text{\AA}^{-1}$  for *ortho*-deuterium and *para*-hydrogen, respectively. Since the memory kernel depends on the value of the  $F^\kappa(q, t)$  itself the solution must be obtained self-consistently. The initial guess for the memory kernel was taken to be equal to the fast binary portion. The integro-differential equations were solved using a fifth-order Gear predictor-corrector algorithm.<sup>56</sup> Typically, less than 10 iterations were required to converge the correlation function, with an average error smaller than  $10^{-8}$  percent.

The same PIMC simulation runs were used to generate the imaginary time  $\tilde{F}^\kappa(q, \tau)$  and the corresponding covariance matrices. We then used the L-curve method to determine the optimal value of the regularization parameter,  $\alpha_q$ . In all the results shown below the value of  $\alpha_q$  ranged between 5 to 20 depending on the value of  $q$  (the results were not found to be very sensitive to the value of  $\alpha_q$  within a reasonable range  $\alpha_q = 1 – 50$ ). The plots of  $\log[-S_q(S(q, \omega))]$  vs.  $\log \chi_q^2$  for all values of  $q$  result in a very sharp L-shape curves, indicating the high quality of the PIMC data.

### B. Liquid *ortho*-deuterium

The results for the Kubo transform of the intermediate scattering function for liquid *ortho*-deuterium obtained from the QMCT and the MaxEnt method are shown in the left panels of Fig. 1 for several values of  $q$ . The right panels of Fig. 1 show the binary and mode-coupling portions of the memory kernel obtained from the QMCT for the same values of  $q$ . The MaxEnt results were generated from  $S(q, \omega)$  by taking the Fourier transform of  $S(q, \omega)$  divided by the proper frequency factor to “Kubo” the real time correlation function.

The most striking result is the discrepancy between the QMCT and the MaxEnt result observed at intermediate and long times for all values of  $q \leq q_{max}$ , where  $q_{max} \approx 2\text{\AA}^{-1}$  is the value of  $q$  where  $S(q)$  reaches its first maximum (upper panel of Fig. 1). The agreement between the QMCT which is exact to order  $t^6$  and the MaxEnt results at short times is expected. However, the MaxEnt result fails to reproduce the proper oscillatory behavior observed in  $F^\kappa(q, t)$  that gives rise to a peak in  $S(q, \omega)$  at a finite frequency (see Fig. 2 below), signifying the existence of collective coherent excitations in liquid *ortho*-deuterium. Common to both approaches is that as  $q$  approaches  $q_{max}$  the decay rate of the Kubo transform of the intermediate scattering function decreases giving rise to a quantum mechanical de Gennes narrowing of the dynamic structure factor (see Fig. 2 below). In addition,

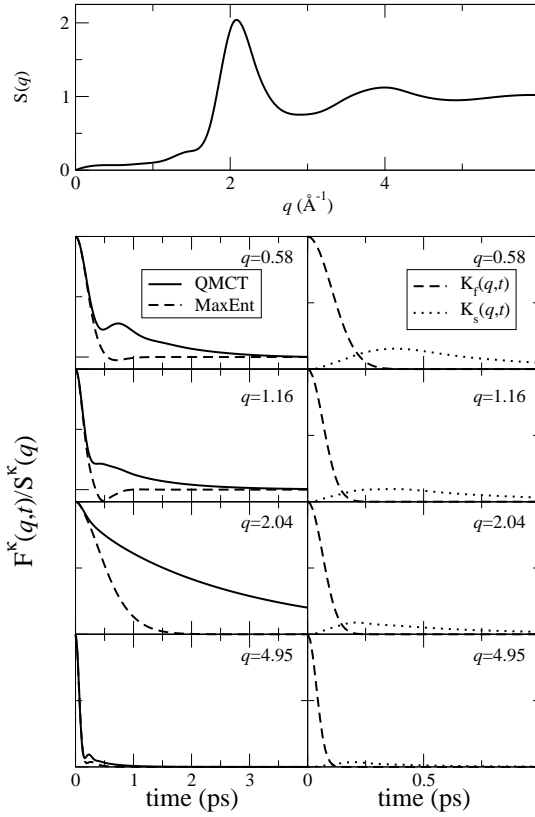


FIG. 1: Plots of the static structure factor (upper panel), the Kubo transform of the intermediate scattering function (left panels), and the Kubo transform of the quantum binary and mode-coupling portions of the memory kernel (right panels) for liquid *ortho*-deuterium. The values of  $q$  indicated in the panels are in units of  $\text{\AA}^{-1}$ .

we observed an increase in the decay rate of  $F^\kappa(q,t)$  at high values of  $q$ , where the two approaches yield nearly identical results on a sub-picosecond timescale.

The results shown in Fig. 1 are the first application of the self-consistent quantum mode-coupling theory described in section II and suggested in Ref. 16. As clearly can be seen in the right panels of Fig. 1 the contribution of the quantum mode-coupling portion of the memory kernel is significant for all values of  $q$  below  $q_{max}$ , while at the highest value of  $q$  shown the contribution of  $K_m^\kappa(q,t)$  is negligible. This is consistent with results obtained for classical dense fluids,<sup>36,37,38</sup> signifying the need to include the long time portion of the memory kernel.

To better understand the origin of the discrepancy between the QMCT and the MaxEnt result for  $F^\kappa(q,t)$  we have compared the results for  $S(q,\omega)$  to the experimental results of Mukherjee *et al.*<sup>26</sup> for several values of  $q$ . The agreement between the experimental results<sup>24,26</sup> and the QMCT is excellent. In particular the theory captures the position of both the low and high intensity peaks and their width for nearly all wavevectors shown. The fact that for limiting cases the QMCT some-

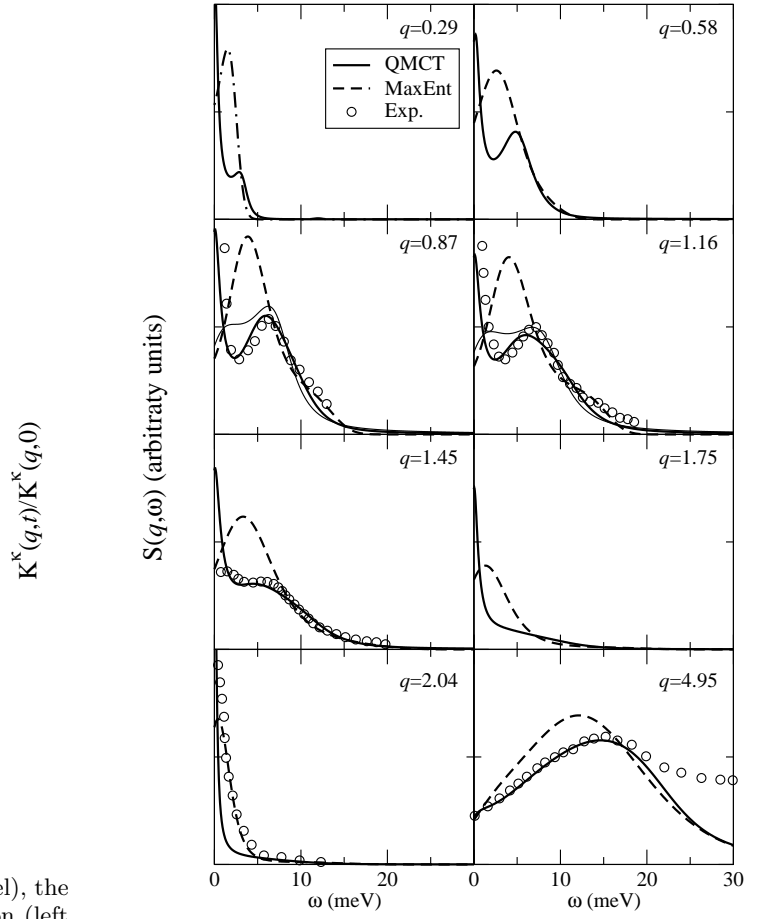


FIG. 2: A plot of the dynamic structure factor of liquid *ortho*-deuterium for several values of  $q$  (in units of  $\text{\AA}^{-1}$ ). The thick solid and dashed lines are QMCT and MaxEnt results , respectively. The thin solid line is the result of QVM,<sup>18</sup> and open circles are the experimental results.<sup>26</sup>

what underestimates the width of the low intensity peak maybe attributed to the broadening associated with the instrumental resolution.<sup>26</sup> This is certainly the case at  $q_{max}$  where the result of the QMCT, which is in excellent agreement with the result obtained from QVM (not shown),<sup>18</sup> underestimates the width of the single low frequency peak. The overall good agreement between the QMCT and the experiments is remarkable since our previous study based on the quantum viscoelastic approach failed to reproduce the low intensity peak associated with long time dynamics (see thin solid line in Fig. 1). Thus, the inclusion of the quantum mode-coupling portion to the memory kernel is important to properly describe long time phenomena. In order to test the accuracy of the approximation for the vertex given by Eq. (18) we have replaced it with its classical limit.<sup>36</sup> The results for the low frequency part of  $S(q,\omega)$  (not shown) are in poor agreement with the experiments. In particular the low intensity peak is absent at intermediate values of  $q$ , and the higher frequency peak is somewhat shifted.

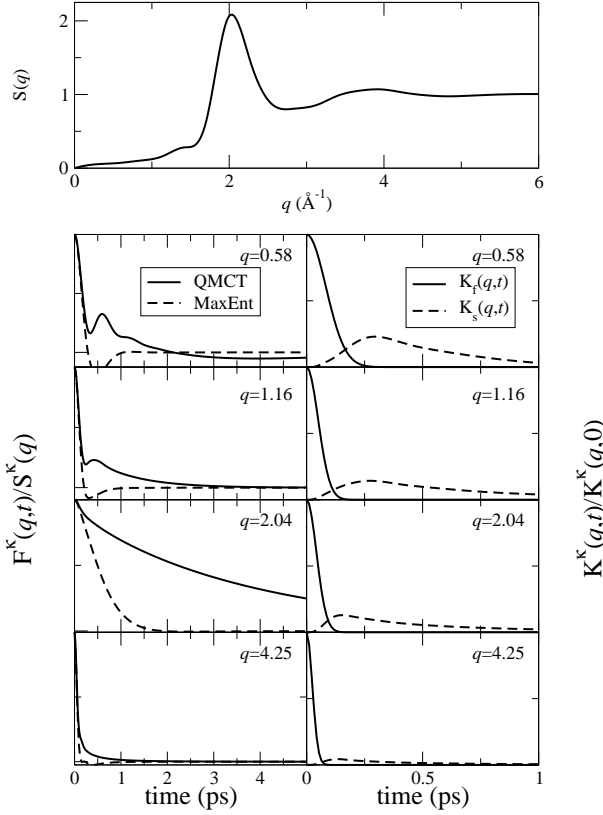


FIG. 3: Plots of the static structure factor (upper panel), the Kubo transform of the intermediate scattering function (left panels), and the Kubo transform of the quantum binary and mode-coupling portions of the memory kernel (right panels) for liquid *para*-hydrogen. The values of  $q$  indicated in the panels are in units of  $\text{\AA}^{-1}$ .

Turning to the MaxEnt results for  $S(q, \omega)$ , it becomes obvious why MaxEnt fails to provide a quantitative description of the density fluctuations in liquid *ortho*-deuterium. It is well known that the MaxEnt approach fails when several timescales arise in a problem. This is clearly the case here where the MaxEnt approach predicts a single frequency peak instead of two, at a position that is approximately the averaged position of the two experimental peaks. Only when the dynamics are characterized by a single relaxation time, like the case at  $q_{\max}$ , the MaxEnt approach provides quantitative results. On the other hand, MaxEnt provides quantitative results for the short time dynamics as reflected in the width of the finite frequency peak in  $S(q, \omega)$  (see also the discussion in Fig. 1).

### C. Liquid *para*-hydrogen

Recently, Zoppi *et al.*<sup>51</sup> have reported a PIMC simulation study of the microscopic structure factor of liquid *para*-hydrogen using the Silvera-Goldman potential.

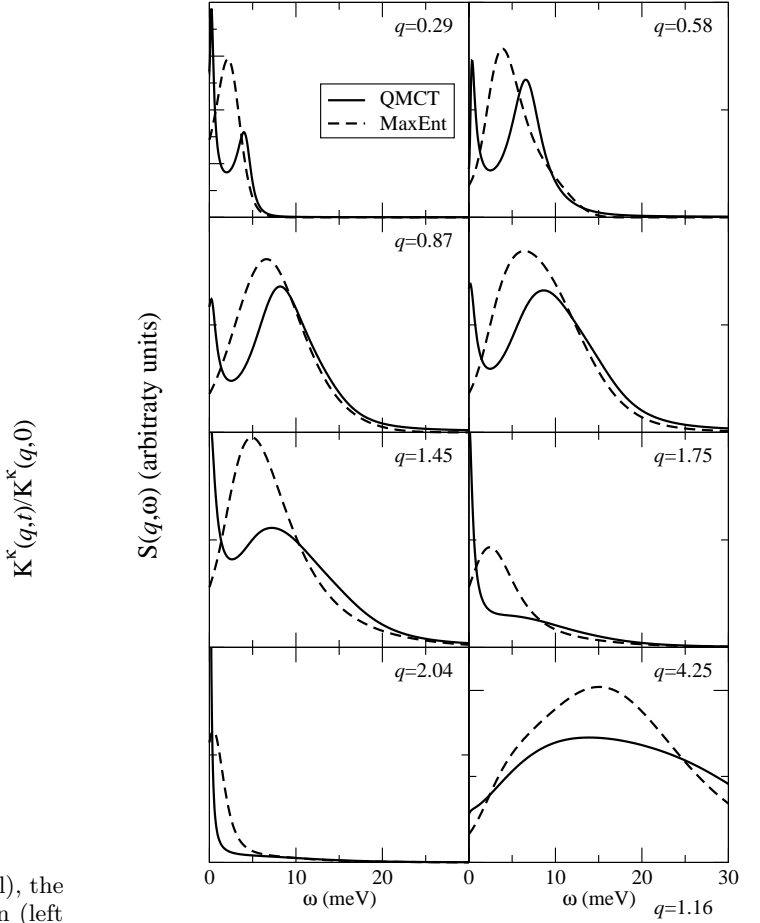


FIG. 4: A plot of the dynamic structure factor of liquid *para*-hydrogen for several values of  $q$  (in units of  $\text{\AA}^{-1}$ ). The solid and dashed lines are QMCT and MaxEnt results, respectively.

Their conclusion was that the differences observed for  $S(q)$  between the simulations and the experiments are “too large to be real.” Their line of reasoning was that the model and PIMC simulations that were successful in deuterium should provide quantitative results for hydrogen as well. The major point of their paper was that the experimental results on *para*-hydrogen are “not sufficiently reliable to serve as a reference for theoretical calculations.”<sup>51</sup> We therefore limit the discussion of this subsection to collective density fluctuations in liquid *para*-hydrogen studied using the QMCT and MaxEnt method only.

In Fig. 3 we show the results for the Kubo transform of the intermediate scattering function for liquid *para*-hydrogen obtained from the QMCT and the MaxEnt method (left panels) for several values of  $q$ . The right panels of Fig. 3 show the binary and mode-coupling portions of the memory kernel obtained from the QMCT for the same values of  $q$ . The agreement between the QMCT and the MaxEnt result is good at short times. Both

approaches capture the quantum mechanical de Gennes narrowing associated with the decrease in the decay rate of the Kubo transform of the intermediate scattering function as  $q$  approaches  $q_{max}$ . In addition both capture the increase in the decay rate of  $F^\kappa(q, t)$  at high values of  $q$  where the two yield nearly identical results. However, similar to the case of liquid *ortho*-deuterium, at intermediate and long times when  $q \leq q_{max}$  the results deviate markedly from each other.

The QMCT results show pronounced oscillatory behavior in  $F^\kappa(q, t)$  that gives rise to a peak in  $S(q, \omega)$  at a finite frequency (see Fig. 4 below). Similar oscillation with a smaller amplitude were also observed in our previous study using the QVM.<sup>17</sup> However, at low values of  $q$  the long time decay of  $F^\kappa(q, t)$  is quite different compared with the QVM results (not shown), signifying the contribution of the quantum mode-coupling portion of the memory kernel for all values of  $q$  below  $q_{max}$ , as can be seen in right panels of Fig. 3. As  $q$  approaches  $q_{max}$  the agreement between the QMCT and the QVM becomes quantitative.

It is interesting to note that the agreement between the QMCT and the MaxEnt method is excellent for the self-transport in *para*-hydrogen,<sup>43</sup> while the results for the dynamic structure factor plotted in Fig. 4 show significant deviations between the two approaches. Most likely the discrepancy results from multiple frequency peaks in  $S(q, \omega)$ . MaxEnt is nearly quantitative as long as  $S(q, \omega)$  is characterized by a single peak. Namely, at high  $q$  values where the decay of  $F^\kappa(q, t)$  is on a sub-picosecond timescale, and at  $q$  values near  $q_{max}$ .

## V. CONCLUSIONS

The problem of calculating collective density fluctuations in quantum liquids has been revisited. Two techniques have been applied to study the dynamic structure factor in liquids *ortho*-deuterium and *para*-hydrogen: The self-consistent quantum mode-coupling theory and the numerical maximum entropy analytic continuation approach. While it is hard to make a comparison between the predictions made by the two approaches and

experiments for liquid *para*-hydrogen,<sup>51</sup> such a comparison can be made for liquid *ortho*-deuterium. We find that the results obtained using the QMCT for collective density fluctuations are in excellent agreement with the experiments on liquid *ortho*-deuterium for a wide range of  $q$  values. On the other hand the results obtained using the MaxEnt approach deviate from the experiments for nearly the entire relevant wavevector range. Failure of the MaxEnt result was attributed to the presence of two peaks in  $S(q, \omega)$ . Improvements of the MaxEnt, such as including real time dynamics in the inversion of the singular integral, may provide more accurate results.

The excellent agreement between our QMCT and the experiments for liquid *ortho*-deuterium is an encouraging indicator of the accuracy of the QMCT. The fact that our QMCT captures the position of both the low and high intensity peaks in the dynamic structure factor and their width for nearly all wavevectors studied is an important result, since our previous studies in which we invoked a single relaxation time for the memory kernel of the QGLE (the QVM) failed to reproduce the low frequency peak.<sup>14,17,18</sup> It is the self-consistent treatment of the mode-coupling portion of the memory kernel that accounts for a proper description of the intermediate to long time dynamics in these systems, and the proper treatment of the vertex in the memory kernel.

The agreement between the QMCT and the experimental results for liquid *ortho*-deuterium emphasize the need for better experiments on liquid *para*-hydrogen. But liquid *para*-hydrogen is not the only system that can be addressed using the QMCT. Future work in other directions, including the dynamic properties of liquid helium, is currently underway.

## VI. ACKNOWLEDGMENTS

This work was supported by The Israel Science Foundation founded by the Israel Academy of Sciences and Humanities (grant number 31/02-1 to E.R.). D.R.R. is an Alfred P. Sloan Foundation Fellow and a Camille Dreyfus Teacher-Scholar.

<sup>1</sup> P. Nozieres and D. Pines, *The Theory of Quantum Liquids* (Perseus, 1999).

<sup>2</sup> G. D. Mahan, *Many-Particle Physics* (Plenum, 2000).

<sup>3</sup> M. Jarrell and J. E. Gubernatis, *Phys. Rep.* **269**, 134 (1996).

<sup>4</sup> G. Krilov, E. Sim, and B. J. Berne, *Chem. Phys.* **268**, 21 (2001).

<sup>5</sup> J. E. Gubernatis, M. Jarrell, R. N. Silver, and D. S. Silvia, *Phys. Rev. B* **44**, 6011 (1991).

<sup>6</sup> C. E. Creffield, E. G. Klepfish, E. R. Pike, and S. Sarkar, *Phys. Rev. Lett.* **75**, 517 (1995).

<sup>7</sup> E. Gallicchio and B. J. Berne, *J. Chem. Phys.* **101**, 9909 (1994).

<sup>8</sup> E. Gallicchio and B. J. Berne, *J. Chem. Phys.* **105**, 7064 (1996).

<sup>9</sup> E. Gallicchio, S. A. Egorov, and B. J. Berne, *J. Chem. Phys.* **109**, 7745 (1998).

<sup>10</sup> S. A. Egorov, E. Gallicchio, and B. J. Berne, *J. Chem. Phys.* **107**, 9312 (1997).

<sup>11</sup> E. Rabani, G. Krilov, and B. J. Berne, *J. Chem. Phys.* **112**, 2605 (2000).

<sup>12</sup> E. Sim, G. Krilov, and B. J. Berne, *J. Phys. Chem.* **105**, 2824 (2001).

<sup>13</sup> M. Boninsegni and D. M. Ceperley, *J. Low Temp. Phys.*

- <sup>104</sup> **339** (1996).
- <sup>14</sup> E. Rabani and D. R. Reichman, *Phys. Rev. E* **65**, 036111 (2002).
- <sup>15</sup> D. R. Reichman and E. Rabani, *Phys. Rev. Lett.* **87**, 265702 (2001).
- <sup>16</sup> E. Rabani and D. R. Reichman, *J. Chem. Phys.* **116**, 6271 (2002).
- <sup>17</sup> D. R. Reichman and E. Rabani, *J. Chem. Phys.* **116**, 6279 (2002).
- <sup>18</sup> E. Rabani and D. R. Reichman, *Europhys. Lett.* **60**, 656 (2002).
- <sup>19</sup> M. Zoppi, L. Uliivi, M. Santoro, M. Moraldi, and F. Barocchi, *Phys. Rev. B* **53**, R1935 (1996).
- <sup>20</sup> F. J. Bermejo, B. Fak, S. M. Bennington, R. Fernandez-Perea, C. Cabrillo, J. Dawidowski, M. T. Fernandez-Diaz, and P. Verkerk, *Phys. Rev. B* **60**, 15154 (1999).
- <sup>21</sup> F. J. Bermejo, K. Kinugawa, C. Cabrillo, S. M. Bennington, B. Fak, M. T. Fernandez-Diaz, P. Verkerk, J. Dawidowski, and R. Fernandez-Perea, *Phys. Rev. Lett.* **84**, 5359 (2000).
- <sup>22</sup> M. Zoppi, D. Colognesi, and M. Celli, *Europhys. Lett.* **53**, 39 (2001).
- <sup>23</sup> M. Celli, D. Colognesi, and M. Zoppi, *Phys. Rev. E* **66**, 021202 (2002).
- <sup>24</sup> F. J. Bermejo, F. J. Mompean, M. Garcia Hernandez, J. L. Martinez, D. Martinmarero, A. Chahid, G. Senger, and M. L. Ristig, *Phys. Rev. B* **47**, 15097 (1993).
- <sup>25</sup> M. Zoppi, U. Bafile, E. Guarini, F. Barocchi, R. Magli, and M. Neumann, *Phys. Rev. Lett.* **75**, 1779 (1995).
- <sup>26</sup> M. Mukherjee, F. J. Bermejo, B. Fak, and S. M. Bennington, *Europhys. Lett.* **40**, 153 (1997).
- <sup>27</sup> G. Biroli and O. Parcollet, *Phys. Rev. B* **65**, 094414 (2002).
- <sup>28</sup> M. P. Kennett, C. Chamon, and J. W. Ye, *Phys. Rev. B* **64**, 224408 (2001).
- <sup>29</sup> L. F. Cugliandolo and G. Lozano, *Phys. Rev. Lett.* **80**, 4979 (1998).
- <sup>30</sup> L. F. Cugliandolo and G. Lozano, *Phys. Rev. B* **59**, 915 (1999).
- <sup>31</sup> R. Zwanzig, in *Lectures in Theoretical Physics*, volume III, page 135 (Wiley, New York, 1961).
- <sup>32</sup> H. Mori, *Prog. Theor. Phys.* **33**, 423 (1965).
- <sup>33</sup> H. Mori, *Prog. Theor. Phys.* **34**, 399 (1965).
- <sup>34</sup> B. J. Berne and G. D. Harp, *Adv. Chem. Phys.* **17**, 63 (1970).
- <sup>35</sup> R. Kubo, M. Toda, and N. Hashitsume, *Statistical Physics II*, Solid State Sciences (Springer, Berlin, 1995), second edition.
- <sup>36</sup> U. Balucani and M. Zoppi, *Dynamics of the Liquid State* (Oxford, New York, 1994).
- <sup>37</sup> J. P. Boon and S. Yip, *Molecular Hydrodynamics* (McGraw Hill, New York, 1980).
- <sup>38</sup> J. P. Hansen and I. R. McDonald, *Theory of Simple Liquids* (Academic Press, San Diego, 1986).
- <sup>39</sup> S. H. Chong and F. Hirata, *Phys. Rev. E* **58**, 7296 (1998).
- <sup>40</sup> D. R. Reichman, P. N. Roy, S. Jang, and G. A. Voth, *J. Chem. Phys.* **113**, 919 (2000).
- <sup>41</sup> H. W. Jackson and E. Feenberg, *Rev. Mod. Phys.* **34**, 686 (1962).
- <sup>42</sup> E. Rabani and D. R. Reichman, *J. Phys. Chem. B* **105**, 6550 (2001).
- <sup>43</sup> E. Rabani, D. R. Reichman, G. Krilov, and B. J. Berne, *Proc. Natl. Acad. Sci. USA* **99**, 1129 (2002).
- <sup>44</sup> B. J. Berne, *J. Stat. Phys.* **43**, 911 (1986).
- <sup>45</sup> B. J. Berne and D. Thirumalai, *Ann. Rev. Phys. Chem.* **37**, 401 (1986).
- <sup>46</sup> J. Skilling, editor, *Maximum Entropy and Bayesian Methods* (Kluwer, Cambridge, England, 1989).
- <sup>47</sup> C. L. Lawson and R. J. Hanson, *Solving Least Squares Problems* (Society for Industrial and Applied Mathematics, 1995).
- <sup>48</sup> P. Sindzingre, D. M. Ceperley, and M. L. Klein, *Phys. Rev. Lett.* **67**, 1871 (1991).
- <sup>49</sup> M. Pavese and G. A. Voth, *Chem. Phys. Lett.* **249**, 231 (1996).
- <sup>50</sup> K. Kinugawa, *Chem. Phys. Lett.* **292**, 454 (1998).
- <sup>51</sup> M. Zoppi, M. Neumann, and M. Celli, *Phys. Rev. B* **65**, 092204 (2002).
- <sup>52</sup> D. Scharf, G. Martyna, and M. L. Klein, *J. Low. Temp. Phys.* **19**, 365 (1993).
- <sup>53</sup> I. F. Silvera and V. V. Goldman, *J. Chem. Phys.* **69**, 4209 (1978).
- <sup>54</sup> I. F. Silvera, *Rev. Mod. Phys.* **52**, 393 (1980).
- <sup>55</sup> E. L. Pollock and D. M. Ceperley, *Phys. Rev. B* **30**, 2555 (1984).
- <sup>56</sup> M. P. Allen and D. J. Tildesley, *Computer Simulation of Liquids* (Clarendon, Oxford, 1987).